Powder Technology 297 (2016) 183–192

Contents lists available at ScienceDirect

Powder Technology

journal homepage: www.elsevier.com/locate/powtec

Synthesis and characterisation of advanced ball-milled Al-Al_2O_3 nanocomposites for selective laser melting

Quanquan Han, Rossitza Setchi *, Sam L. Evans

School of Engineering, Cardiff University, Cardiff CF24 3AA, UK

ARTICLE INFO

Article history:
Received 14 January 2016
Received in revised form 2 April 2016
Accepted 9 April 2016
Available online 13 April 2016

Keywords:
Al-Al_2O_3 nanocomposite
Selective laser melting
High-energy ball milling
Flowability
Vickers micro-hardness

ABSTRACT

Selective laser melting (SLM) offers significant potential for the manufacture of the advanced complex-shaped aluminium matrix composites (AMCs) used in the aerospace and automotive domains. Previous studies have indicated that advanced composite powders suitable for SLM include spherical powders with homogeneous reinforcement distribution, a particle size of <100 μm and good flowability (Carr index < 15%); however, the production of such composite powders continues to be a challenge. Due to the intensive impacts of grinding balls, the high-energy ball-milling (HEBM) process has been employed to refine Al particles and disperse the nano Al_2O_3 reinforcements in the Al matrix to improve their mechanical properties. Notwithstanding, the specific characteristics of ball-milled powders for SLM and the effect of milling and pause duration on the fabrication of composite powders have not previously been investigated. The aim of this study was to synthesise Al-4 vol.% Al_2O_3 nano-composite powders using HEBM with two different types of milling and pause combinations. The characteristics of the powders subjected to up to 20 h of milling were investigated. The short milling (10 min) and long pause (15 min) combination provided a higher yield (66%) and narrower particle size distribution range than long milling (15 min) and a short pause (5 min). The nano Al_2O_3 reinforcements were observed to be dispersed uniformly after 20 h of milling, and the measured Carr index of 13.2% indicated that the ball-milled powder offered good flowability. Vickers micro-hardness tests indicated that HEBM significantly improved the mechanical properties of the ball-milled powders.

1. Introduction

Metal matrix composites (MMCs) offer high specific strength and good wear resistance with various applications in the aerospace, defence and automotive industries [1–3]. Amongst the MMCs, aluminium-based matrix composites (AMCs) are increasingly being used due to their light weight, high specific stiffness, excellent wear resistance and controllable expansion coefficient [4–6]. A wide range of reinforcement particulates such as Al_2O_3, SiC, B_4C, AlN, TiC, TiO_2 and TiB_2 have been used [7], but compared to other reinforcements, nano-scale Al_2O_3 particulates are capable of improving both their wear behaviour and high temperature properties without introducing any undesirable phases and are therefore widely used in AMCs [8].

Studies have shown that the strength of Al-Al_2O_3 nanocomposites increases with the volume fraction of nano Al_2O_3; however, the strengthening effect is found to level off when the volume fraction is above 4 vol.%, which is attributed to the clustering of nano Al_2O_3 particulates [9,10]. Therefore, recent research has concentrated on the development of advanced Al-4 vol.% Al_2O_3 nanocomposites. Nonetheless, the applications of Al-Al_2O_3 composites have been limited to very specific areas such as aerospace and defence due to their high processing costs and the lack of a feasible fabrication method [1]. Compared to traditional manufacturing technologies such as casting, extrusion and computer numerical control (CNC) machining, additive layer manufacturing (ALM) has become one of the most rapidly developing advanced manufacturing technologies in the world. ALM is based on the layer-by-layer manufacturing principle and provides an integrated way of manufacturing three-dimensional (3D) complex-shaped components from computer-aided design (CAD) files [11,12]. Amongst the ALM techniques, selective laser melting (SLM) is being used widely to manufacture 3D-complex shaped metallic parts [13]. Therefore, the SLM of advanced Al-Al_2O_3 nanocomposites is expected to offer significant potential in the fabrication of advanced customised engineering components such as automobile engine pistons, cylinder liners and brake drums [14].

On the other hand, a metallic powder suitable for SLM should generally offer spherical morphology, good flowability and a small particle size (1–100 μm) with a narrow particle size distribution range. Studies have shown that hot-pressed parts manufactured using Al-Al_2O_3 powder with an average grain size of 50 nm provide a yield strength of 661 MPa [10]. Therefore, it is crucial to produce this type of advanced

* Corresponding author.
E-mail address: Setchi@cardiff.ac.uk (R. Setchi).

http://dx.doi.org/10.1016/j.powtec.2016.04.015

Al-4 vol.% Al_2O_3 nanocomposite powder for use in the SLM process. High-energy ball milling (also known as mechanical milling) has proved to be a simple and effective technique to refine particle grain size (~100 nm) and disperse reinforcement materials homogeneously in a metal matrix [15–17]. Another advantage of high-energy ball milling lies in its ability to produce bulk quantities of solid-state materials using simple equipment at room temperature.

Accordingly, the aim of this work is to synthesize an advanced Al-Al_2O_3 nanocomposite powder for SLM using HEBM with two different types of milling and pause combinations. This study aims to expand the potential applications of the SLM process in producing advanced MMCs components. Compared to previous studies, the main novelty of this work is that it investigated the effect of milling and pause duration on the fabrication of ball-milled powders for SLM, which has not been researched in other studies. The systematic analytical methods used to evaluate the characteristics of the ball-milled powders suitable for SLM was considered to be another novelty of this work. The employed analytical techniques and advanced metrology methods in this study can also be used to explore the synthesis of other new materials used for SLM.

2. Related work

The high-energy ball-milling process was initially employed to produce oxide dispersion strengthened (ODS) nickel and iron-based super alloys for use in the aerospace industry [18]. After almost 40 years of development, the technique was shown to be capable of producing different types of advanced materials, including amorphous alloy powders, nanocrystalline powders, and composite and nanocomposite powders [19].

Amongst the early studies of this technique, Prabhu et al. [20] employed a SPEX mill to synthesize Al-Al_2O_3 composite powders with volume fractions of 20%, 30% and 50% and found that the Al_2O_3 reinforcement materials were distributed homogeneously in the Al matrix after 20 h of milling at a ball-to-powder weight ratio of 10:1. Zebarjad and Sajjadi [1] investigated the physical and mechanical properties of the aluminium-alumina composites produced by the mechanical milling method and found that the milling time had a significant effect on the mechanical and physical properties of the composites; however, increasing the milling time was shown to have no significant effect on the properties when the steady state was achieved. In another study of the effect of milling on composite microstructures [21], it was found that at the beginning of the process the powders tended to absorb iron, and the trend gradually decreased until the steady state. Moreover, the increase of milling time contributed to the formation of fine alumina particulates and their uniform distribution performance. Tousi et al. [16] employed high-energy milling to produce Al-20 wt.% Al_2O_3 composite powder; the reinforcement material added comprised submicron α-alumina particles. Consequently, the distribution of the alumina particles in the Al matrix was homogeneous when the steady state was achieved, which increased the hardness of the milled powder.

More recently, Khorshid et al. [22] investigated the mechanical properties of aluminium matrix composites reinforced by two sizes of alumina particles (35 nm and 0.3 μm) by wet attrition milling, and found that the hardness and yield strength improved with the increased amount of alumina; nonetheless, when the fraction exceeded 4 wt.%, both the hardness and strength decreased. Poirier et al. [10] studied the mechanical properties of ball-milled Al-Al_2O_3 nanocomposites and established that the hardness of the composites was five times higher than pure unmilled Al; a decrease in the Al_2O_3 particle size from 400 nm to 4 nm led to a 11% increase in the hardness of the composites. Su et al. [23] investigated the processing, microstructure and tensile properties of Al-Al_2O_3 nano composites by ball milling and ultrasonic treatment. They determined that, compared to an aluminium alloy matrix, the ultimate tensile strength and yield strength of the Al-1 wt.% Al_2O_3 composite increased by 37% and 81%, respectively; this can be explained by the grain refinement and homogeneous dispersion of the nano reinforcements.

Nevertheless, none of the aforesaid researchers employed HEBM to produce advanced Al-Al_2O_3 nanocomposite powders suitable for SLM, and further, the effect of milling and pause duration on the fabrication of Al-Al_2O_3 nanocomposites has not been investigated. This study therefore investigated the yield difference when employing two sets of milling and pause time combinations, and explored the characteristics of advanced composite powder following up to 20 h of milling.

3. Materials and procedures

3.1. Raw materials and apparatus

Raw Al and Al_2O_3 powders were obtained from commercial vendors. Raw Al powder (−325 mesh, 99.5%) was acquired from the Alfa Aesar Corporation (Ward Hill, MA), and Al_2O_3 powder (<50 nm particle size) was obtained from Sigma-Aldrich Ltd. (Dorset, UK). Fig. 1a and b show the irregular shape of the raw Al and high surface energy-induced Al_2O_3 clusters. The particle size distribution of the Al and Al_2O_3 were measured using the Malvern Mastersizer3000 (Malvern, U.K.) and Philips CM12 TEM (FEI U.K. Ltd. Cambridge, U.K.), respectively. Fig. 1c shows the average particle size of raw Al and Al_2O_3 powder were 17.1 μm and 10.37 nm, respectively. A laboratory planetary mill with four working stations (PULVERISETTE 5 classic line, Fritsch GmbH, Idar-Oberstein, Germany) was employed to conduct the ball-milling experiments (Fig. 1d) in this study.

3.2. Methods and procedures

A stainless steel bowl was loaded with 200 g Al and 4 vol.% of Al_2O_3 powders with a ball-to-powder weight ratio of 5:1; meanwhile, to identify the effect of the nanoscale Al_2O_3 reinforcements on the ball-milled composite powders, 200 g of Al without Al_2O_3 was loaded into another stainless steel bowl. To prevent excessive cold-welding, 3 wt.% of stearic acid, which functioned as a process control agent (PCA), was added to each bowl. Further, to prevent oxidation during the ball-milling process, the grinding bowls were filled with argon gas, and a lock device was used to gas-tight seal the bowls in the glove box. The milling speed was set at 350 rpm, and the samples were taken out every 4 h for analysis until 20 h of milling had been completed. To investigate the influence of the milling and pause time on the yield and powder characteristics, two sets of experiments were conducted separately; the first set of experiments employed a 15-minute milling and 5-minute pause combination (further referred to in this paper as method 1) while the second experiment involved a 10-minute milling and 15-minute pause combination (method 2).

The composite powder ball-milled for 20 h was subject to sieving to obtain a powder suitable for the SLM process. A standard 170 mesh sieve (90 μm) was employed for this purpose. The weight loss (W_Δ) and yield (φ) can be expressed as:

$$W_\Delta = W_i - W_o \tag{1}$$

$$\varphi = \frac{W_{90}}{W_i} \times 100\% \tag{2}$$

where W_i and W_o denote the weight of input and output after 20 h of milling, respectively, and W_{90} represents the weight of the powders that passed through the sieve with a particle size of <90 μm.

To measure the flow behaviour of the sieved ball-milled powders, the Carr index (CI) was used. The Carr index is the ratio of the difference between the apparent volume and the tapped volume to the apparent

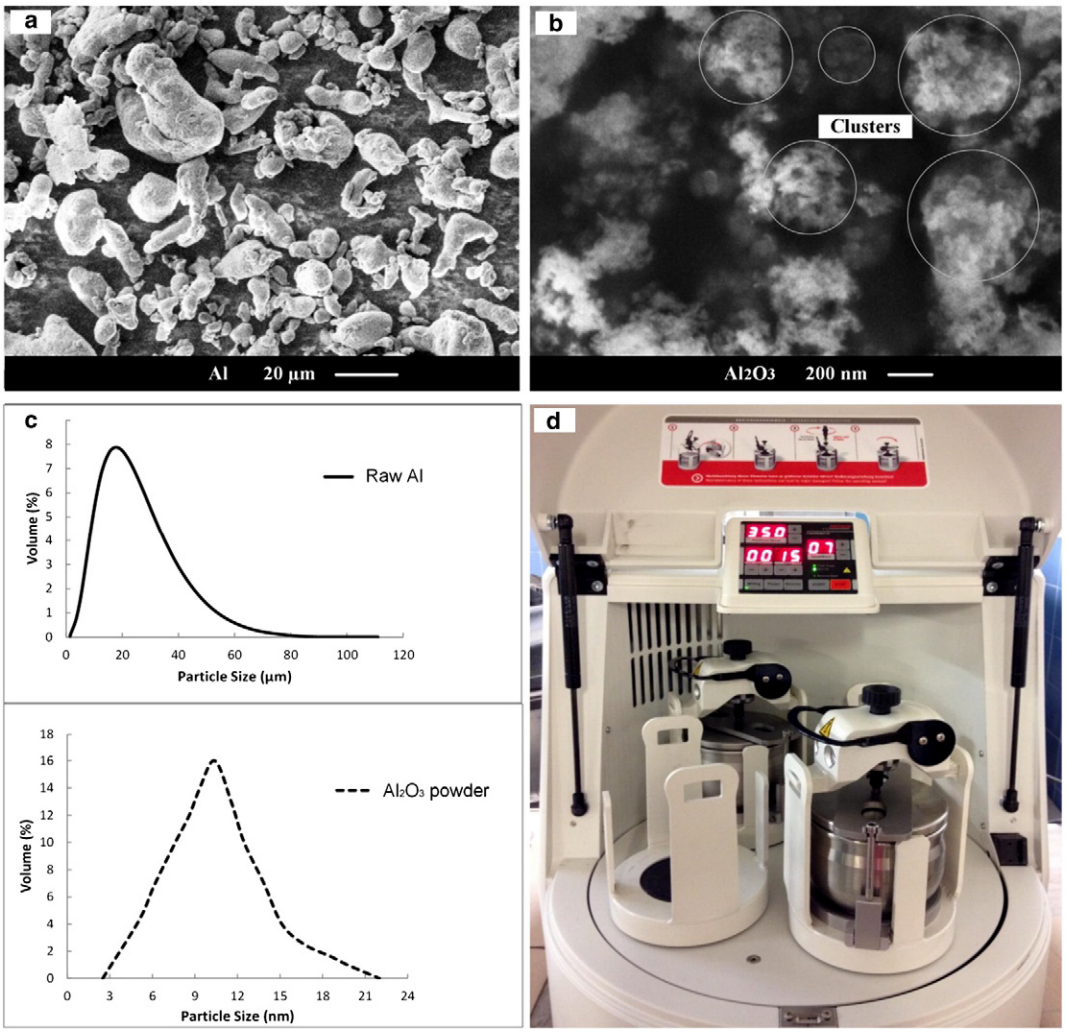

Fig. 1. Raw materials and apparatus: (a) raw Al, (b) nano Al_2O_3, (c) particle size distribution of raw Al and Al_2O_3 powder, (d) the ball mill.

volume, and can be expressed as [24,25]:

$$CI = \frac{V_A - V_T}{V_A} \times 100\% \tag{3}$$

where V_A denotes the apparent volume that results from pouring the powder into a heap or container in the absence of any applied compression, and V_T represents the tapped volume resulting from the application of compression, for example, impact or vibration. Generally, a Carr index of <15% is considered to be an indicator of good flowability while >20% indicates poor flowability [26]. The apparent and tapped volumes of the sieved ball-milled powders were measured in terms of ASTM D7481-09 to calculate the Carr index using a 100 mL standard graduated cylinder.

Other metrology and analytical techniques were employed for phase identification, grain size and uniformity evaluation, flow behaviour analysis and micro-hardness measurement for microstructural changes. More specifically, scanning electron microscopy (SEM) was used to observe the powders' morphology evolution. In addition to phase identification, X-ray powder diffraction (XRD) was also used to evaluate the average grain size when the grain size was <100 nm. The average grain size d can be expressed using the Scherrer equation [27]:

$$d = \frac{0.9\lambda}{\beta \cos\theta} \tag{4}$$

where β and θ denote the full width at half maximum (FWHM) and Bragg angle, respectively, and λ is the wavelength of the X-radiation. Transmission electron microscopy (TEM) together with energy-dispersive X-ray spectroscopy (EDS) was used to evaluate the uniformity of the nanoscale Al_2O_3 in the Al matrix by measuring the atomic and weight percentages of the constituent elements. On the other hand, the weight percentage of the Al elements in the Al-Al_2O_3 composite was determined by

$$W\% = \frac{W_1 + \frac{9}{17} \cdot W_2}{W_1 + W_2} \times 100\% \tag{5}$$

where W_1 and W_2 denote the weight of Al and Al_2O_3 powders, respectively. This indicator can be used to verify the validity of the results from the TEM and EDS analyses.

To investigate the effect of both ball milling and nano Al_2O_3 reinforcements on the powders' mechanical properties, the Al and Al-Al_2O_3 composite ball-milled for 20 h as well as the raw Al powders were separately mounted in carbon-filled phenolic resins. The specimens were polished before micro-hardness testing. The Micro-Vickers Hardness Testing Machine HM-101 (Mitutoyo UK Ltd) was employed to measure the specimens' micro-hardness. The average Vickers hardness of each specimen was determined by measuring four different indentations with an applied load of 50 g.

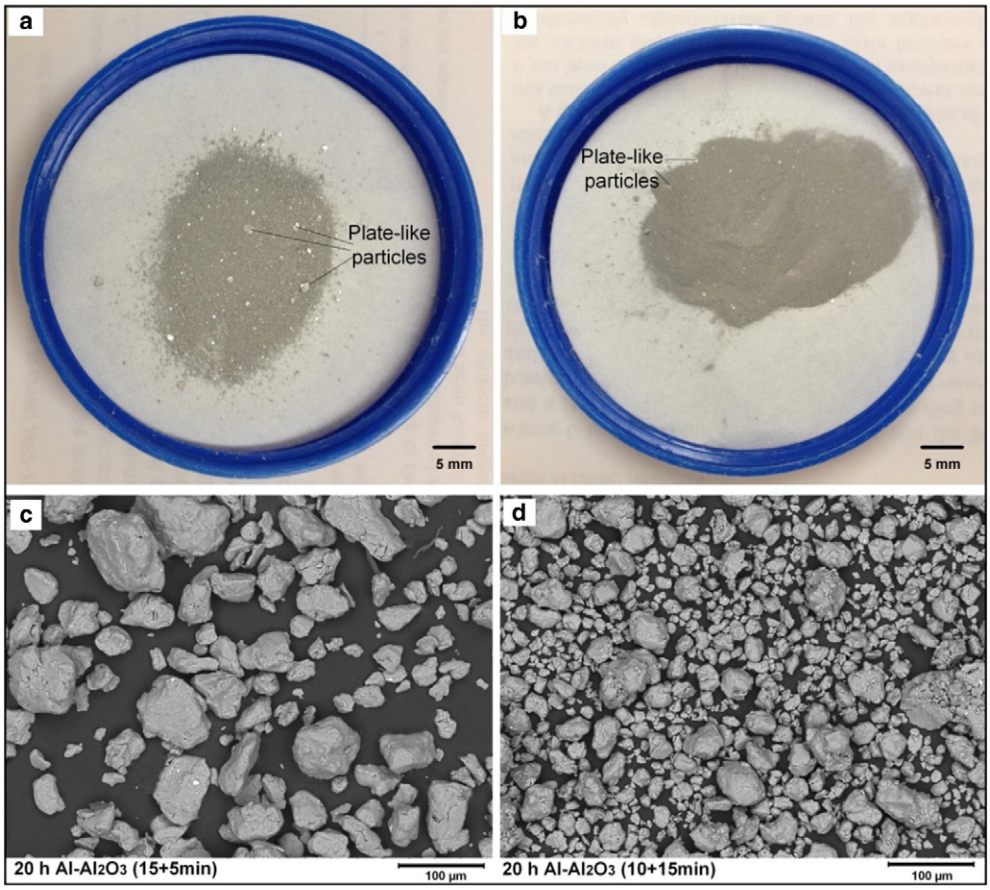

Fig. 2. Two types of composite powder ball-milled for 20 h.

4. Results and discussion

4.1. Particle size distribution and yield evaluation

Fig. 2a and b show two types of Al-4 vol.% Al_2O_3 composite powder ball-milled for 20 h when employing two different combinations of milling and pause duration. More specifically, when the milling and pause time were set at 15 and 5 min, respectively (method 1), some large and plate-like particles formed in the ball-milled composite powder (Fig. 2a), which can be attributed to the agglomeration of the very fine composite powder. Nevertheless, very few plate-like particles were found in the composite powder when employing the 10-minute milling and 15-minute pause combination (method 2, Fig. 2b).

To produce advanced Al-Al_2O_3 nanocomposite powders suitable for the SLM process, both types of composite powder were subject to sieving. The particles that passed through the 170 mesh sieve (≤90 μm) are shown in Fig. 2c and d, that is, Fig. 2c shows the sieved composite powder fabricated by method 1 (15 + 5 min) while Fig. 2d shows the sieved composite powder produced by method 2 (10 + 15 min). Compared to the method 1-produced composite powder, the composite powder produced by method 2 offered a much smaller particle size and more spherical particle shape.

Further, the particle size distribution of the two sieved composite powders was obtained using the Malvern Mastersizer3000 (Fig. 3a). Following ball milling for 20 h, the composite powder from method 1 provided an average particle size of 45 μm with a broad range of particle sizes between 5 and 90 μm while method 2 produced a composite powder exhibiting an average particle size of 25 μm with a much narrower particle size range between 2 and 55 μm. Therefore, from a particle size distribution point of view, the sieved composite powder ball-milled for 20 h from method 2 would be more suitable than the method

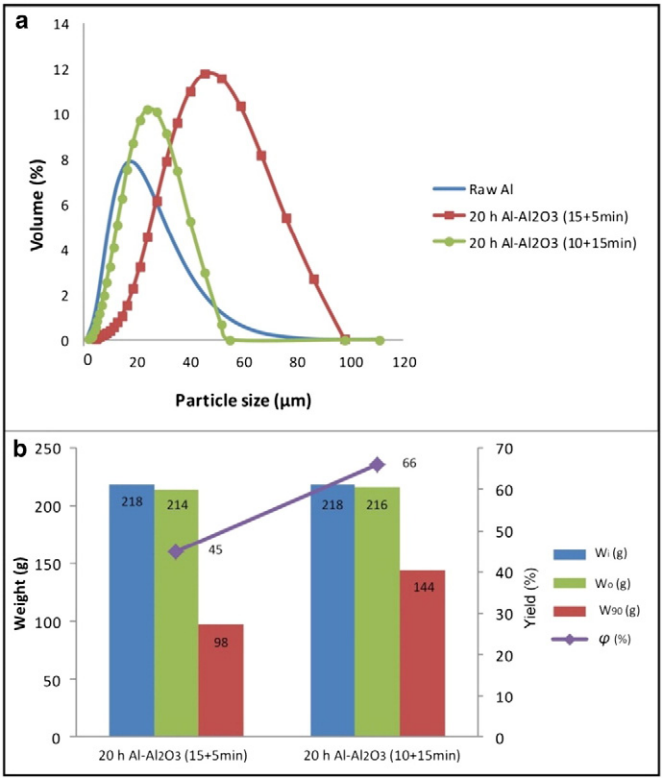

Fig. 3. The particle size distribution and yield of the sieved composite powders.

1-produced composite powder for the SLM process for two reasons. First, small particles tend to provide larger surface areas and thus contribute to a higher laser energy absorption rate during the laser melting stage than large particles, and second, the particles with a narrow range of particle sizes could ensure high dimensional accuracy in each powder layer during the powder deposition stage and further ensure the dimensional accuracy of the final parts.

In addition to particle size distribution, yield was another key factor employed to evaluate the two methods used to produce advanced SLM suitable Al-Al_2O_3 nanocomposites. In both experiments, the weight of the input (W_i) was 218 g, which consisted of 200 g Al, 4 vol.% of Al_2O_3 (12 g) and around 3 wt.% of stearic acid (6 g). When method 1 was employed, the weight of the output (W_o) was approximately 214.5 g compared to 216 g from method 2. Due to the presence of sufficient lubricant, almost no powder was found sticking to the surface of the grinding bowls and balls after 20 h of milling. In terms of Eq. (1), the weight loss (W_Δ) in the two experiments was 3.5 g and 2 g for methods 1 and 2, respectively. Moreover, after sieving, the weights of the particles with a particle size of <90 μm (W_{90}) were 98 g and 144 g, respectively. Yields (φ) of 45% (method 1) and 66% (method 2) can thereby be determined using Eq. (2).

It should be noted that method 1 provided a high weight loss and low yield while method 2 offered a low weight loss and relatively high yield, which can be attributed to the different weights of the stearic acid that remained in the composite powders after 20 h of milling. Indeed, due to the intensive impacts of the grinding balls during ball milling, the temperature in the bowls increased gradually, and when the temperature was over 90 °C, the lubricant (stearic acid) started to volatilise, which led to the welding and agglomeration of the refined composite powder. Generally, a short milling and long pause time combination together with built-in fans could cool the grinding bowls better than a long milling and short pause time combination. Therefore, the weight loss (W_Δ) of 3.5 g and 2 g for methods 1 and 2, respectively, can be primarily attributed to the volatilisation of the stearic acid.

Nonetheless, it should also be noted that a relatively short milling and long pause time combination tends to consume more working time and electrical energy. An understanding of this is crucial for engineers to optimise the process parameters to improve working efficiency when the high-energy ball-milling process is used to produce large quantities of advanced engineering materials.

4.2. SEM morphological evolution and flowability analysis

The morphology of the composite powder was considered to be important to determine whether it would be suitable for SLM as this would affect the powder's flow behaviour in the powder layer deposition stage. Fig. 4 shows the morphological evolution of the Al-Al_2O_3 composites and Al powders following up to 20 h of milling when method 2 was used.

More specifically, Fig. 4a shows the morphology of the composite powder ball milled for 4 h; it can be seen that the welded particles were irregular shapes and had particle sizes of >100 μm, which can be explained by the ductile nature of Al. With the continued milling process, the fracture mechanism was activated, and some large particles were crushed due to intensive impacts, which resulted in morphological changes and particle size reduction (Fig. 4b). When the milling time was increased to 16 h, the fracture phenomenon was more prominent and a considerable number of small particles (particle size around 20 μm) were formed. Meanwhile, some particles exhibited nearly spherical shapes whilst a few large particles remained (Fig. 4c). When the milling time was extended to 20 h (Fig. 4d), the composite powder offered a much narrower particle size range and more nearly spherical particles were formed. In fact, there was no apparent change in the particle size and morphology when the milling time was over 20 h, and this can be attributed to the achieved steady state between the cold-welding and fracture mechanisms. However, Tousi et al. [16] found that the Al-Al_2O_3 composite powder could reach steady state when the milling time was up to 15 h. This can be explained by the employment of process parameters, that is, in the present work, the employed ball-to-powder weight ratio was 5:1 compared to the 15:1 in the literature. A higher ball-to-powder weight ratio could generate more intensive impacts of the grinding balls and thereby shorten the milling time. On the other hand, the higher weight ratio tended to produce a smaller quantity of milled powder in one milling.

To investigate the effect of the added nano Al_2O_3 on the powders' morphological evolution, the morphologies of the Al powder subjected to 8 and 20 h of milling were also examined and are shown in Fig. 4e and f. It can be seen that, compared to the composite powder ball-milled for 8 h, the Al powder ball-milled for 8 h was still in the plastic deformation stage, and cold-welding was the prominent mechanism as most of the particles were plate-like in shape. This can be explained by the fact

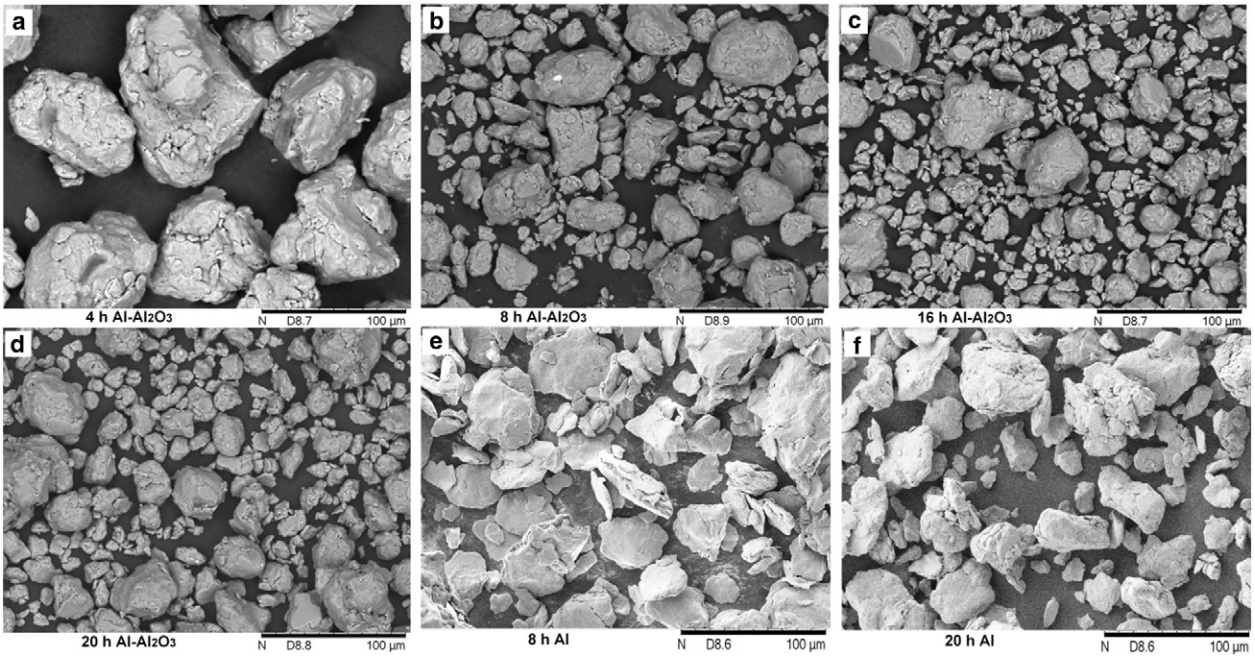

Fig. 4. The morphological evolution of the Al-Al_2O_3 composites and Al powders ball-milled for up to 20 h.

that the added 4 vol.% of nano Al_2O_3 particulates functioned as the grinding media in the composite powder ball-milled for 8 h. Together with the loaded grinding balls, this stimulated and shortened the plastic deformation duration, and the fracture mechanism was activated ahead of 8 h of milling. When both the composite and Al powders ball-milled for 20 h were compared, the former exhibited more spherical shapes and a narrower range of particle size distribution than the latter, which suggested that the former would be more suitable for the SLM process and would offer better flowability.

Composite powders' flowability is considered crucial for the SLM process as it determines the powder's deposition performance. Generally, good-flowing powders generate powder layers with continuous and uniform thickness while poor-flowing powders lead to non-uniform layers, which are detrimental to the dimensional accuracy and mechanical properties of the final parts. The Carr index can be used to evaluate the flow behaviour of advanced ball-milled Al-Al_2O_3 composite powders. As mentioned previously, powders with a Carr index of <15% are considered to have good flowability while a Carr index >20% implies poor flowability.

Fig. 5 shows the measurement results for 55 g of raw Al and the same mass of Al and Al-Al_2O_3 composite powders ball-milled for 20 h. The measured apparent and tapped volumes for the raw Al were 51 mL and 38 mL, respectively. The tapped volume was obtained by tapping the 100 mL cylinder 500 times and measuring the tapped volume to the nearest graduated unit. Using Eq. (3), the Carr index was determined to be 25.5%. Likewise, the measurements of the Al and Al-Al_2O_3 composite powders ball-milled for 20 h were taken, and further, the Carr index values were determined to be 17.5% and 13.2%, respectively.

The results indicated that amongst the three powders, the Al-Al_2O_3 composite powder ball-milled for 20 h exhibited the best flowability followed by the Al ball-milled for 20 h, while the raw Al offered poor flowability with a Carr index of 25.5%. This can be explained by two factors, the first of which is the powder's morphological evolution. Generally, spherical powders tend to have better flowability than non-spherical powders. The morphologies of the raw Al and the Al and Al-Al_2O_3 composite powders ball-milled for 20 h are shown in Figs. 1 and 4, respectively. As shown, some of the composite particles have a nearly spherical shape while most of the Al powder ball-milled for 20 h is equiaxed in shape; the raw Al however exhibits an irregular shape. The second factor is the addition of the stearic acid, which functioned as a lubricant and further improved the flow behaviour of the ball-milled powders by reducing the friction between adjacent particles.

Therefore, it can be concluded that the raw Al powder was likely to be unsuitable for the SLM process because, during the powder layer deposition, a non-uniform layer could be generated, resulting in poor dimensional accuracy of the final parts. Notwithstanding, when employing a combination of 10-minute milling and a 15-minute pause, the produced advanced Al-Al_2O_3 composite powder ball-milled for 20 h not only provided an ideal particle size distribution, but also offered good flowability and was therefore considered to be suitable for the SLM process.

4.3. Phase identification and uniformity evaluation

To investigate contamination and the phases formed during the ball-milling process, the XRD patterns of the composites and Al powders following up to 20 h of milling were measured and are shown in Fig. 6. More specifically, after 20 h of milling, the diffraction patterns of the milled Al still exhibited typical aluminium peaks, but these were broadened, which could be attributed to refinement of the Al grains. It also indicated that the iron elements from the grinding bowl and balls were not present or were below the levels of detection. This finding was in agreement with [27], in which the observed XRD patterns of Al broadened and mean grain size reduced until the milling time was up to 24 h. This phenomenon validated the hypothesis that the ball milling significantly contributed to the grain refinement. Nonetheless, the peaks of the composite powder ball-milled for 20 h exhibited a slightly horizontal offset and relatively weak intensity compared to the 20 hour-milled Al. This can be explained by the fact that the nano Al_2O_3 reinforcements were embedded in the Al matrix, which also broadened the peaks of the composite powder.

It should also be noted that the patterns of the Al_2O_3 powder were not detected in the XRD spectrum, this however was different from the observation elsewhere [20], where the spectrum of nano Al_2O_3 powder was detected in the composite powder's XRD diffraction patterns. This can be attributed to the fact that the employed volume fraction of Al_2O_3 powder in [20] ranged from 20% to 50%, which was much higher than the volume fraction used in the present work (4 vol.%). It can be seen that the measured FWHM of the 20 hour-milled composite powder was larger than that of 20 hour-milled Al, which verified the hypothesis that the added nanoscale Al_2O_3 particulates would serve as the grinding media and accelerate the Al powder grain refinement. The average grain size of the Al and Al-Al_2O_3 composite powders ball-milled for 20 h were determined using Eq. (4) and were 48 nm and 42 nm, respectively. The patterns of the Al-Al_2O_3 composite powder after 4 and 12 h of milling are also shown in Fig. 6, which illustrates that the peaks broadened with the continued milling process.

The uniformity of the nano Al_2O_3 reinforcements in the Al matrix was crucial for the mechanical property improvement of the composite, but the XRD spectrum could not provide more information on this. TEM inspections however did offer a visual and qualitative evaluation. Fig. 7a shows a typical TEM image of Al powder milled for 20 h, and some individual Al grains can be clearly observed. Meanwhile, Fig. 7b shows the TEM image of the composite powder ball-milled for 20 h in which the

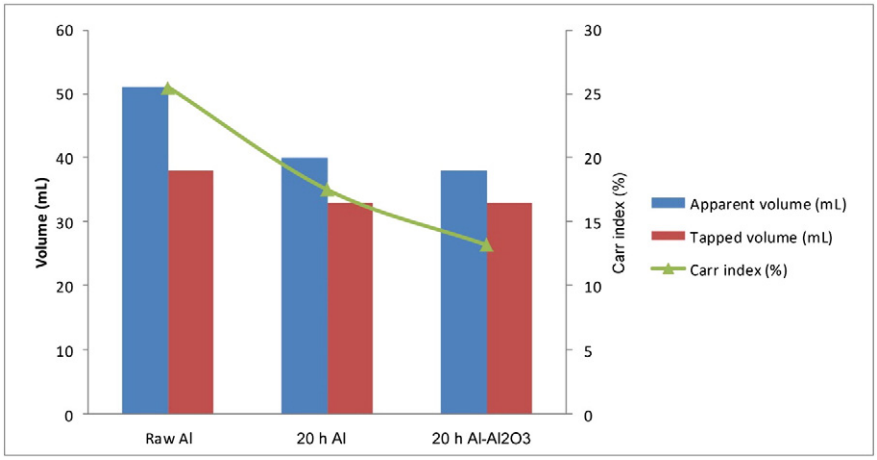

Fig. 5. Flowability measurements and the Carr index.

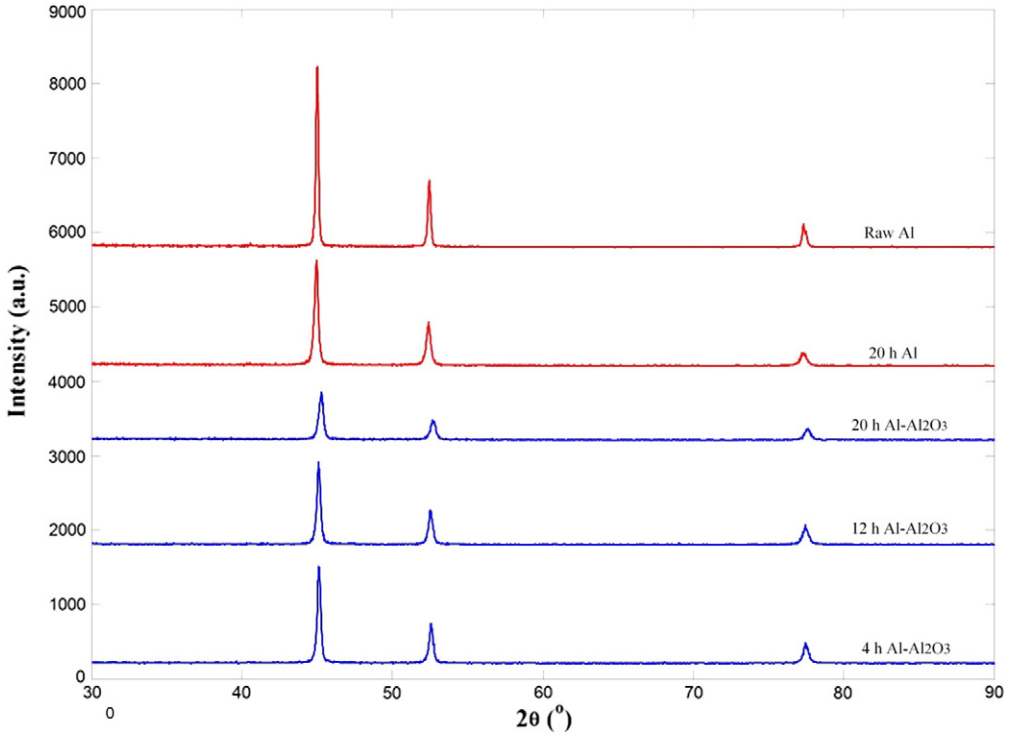

Fig. 6. The XRD patterns of the Al-Al_2O_3 composite and Al powders ball-milled for up to 20 h.

dispersed nano Al_2O_3 particulates were embedded in Al and the original Al grains were split into new grains. This behaviour finally contributed to the improvement in the mechanical properties of the Al-Al2O3 nanocomposite. Another study [9] also found that the nano Al2O3 particulates tended to fill in the gaps between Al powders during powder mixing process. The particulates could pin grain boundaries and give rise to grain-refinement to improve the mechanical properties. It was also reported that when the volume fraction of Al_2O_3 was over 4%, the nano particulates on the grain boundaries would reach saturation and the effect of the nano particulates on grain boundary pinning could diminish and thereby reduce the mechanical properties of the composite.

Indeed, when subjected to external load, the Al matrix bears the major portion of the applied load while the small dispersed particles (Al_2O_3) hinder the motion of the dislocations; plastic deformation is thereby restricted such that yield and tensile strength, as well as hardness, are improved. Even at high temperatures, the strengthening remains and for extended time periods because the dispersed Al_2O_3 particulates are unreactive with the Al matrix.

Nonetheless, it was not easy to quantitatively measure the uniformity of the dispersed nano Al_2O_3 reinforcements in the Al matrix. Compared to the other analytical techniques (e.g. TEM), EDS mapping provided a relatively accurate method to evaluate the uniformity. Fig. 8a shows the measured area of a composite particle while Fig. 8b shows the distribution of the two elements Al and O in the measured image field. It can be seen that the oxygen element from alumina was uniformly distributed in the measured image field, and only Al and O were detected in the EDS spectrum (Fig. 8c).

The atomic and weight fractions of the Al and O elements are shown in Table 1. The weight percentages of the Al and O elements determined using EDS were 97.64% and 2.36%, respectively. As the Al weight

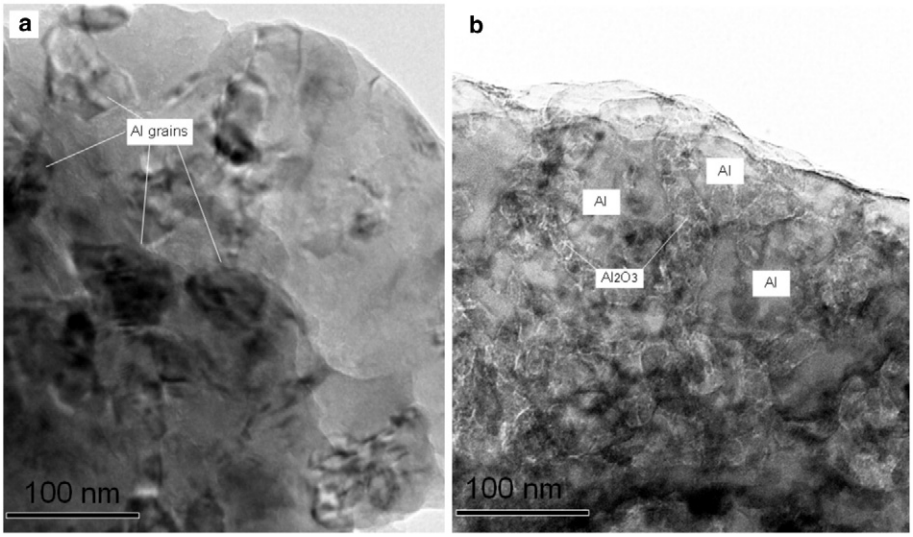

Fig. 7. TEM images of the Al and Al-Al_2O_3 composite powders ball-milled for 20 h.

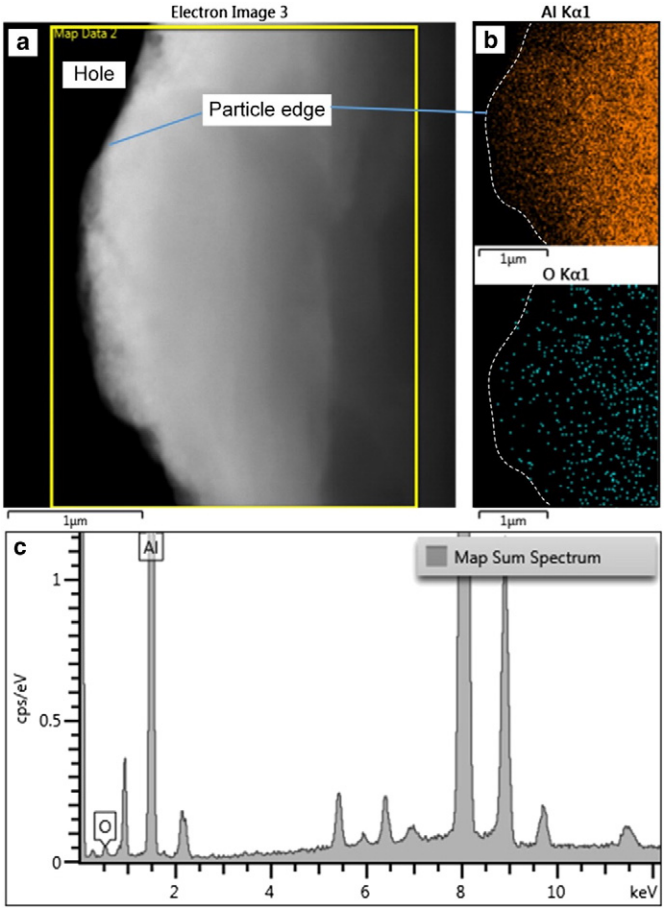

Fig. 8. EDS patterns of the Al-Al_2O_3 composite powder ball-milled for 20 h.

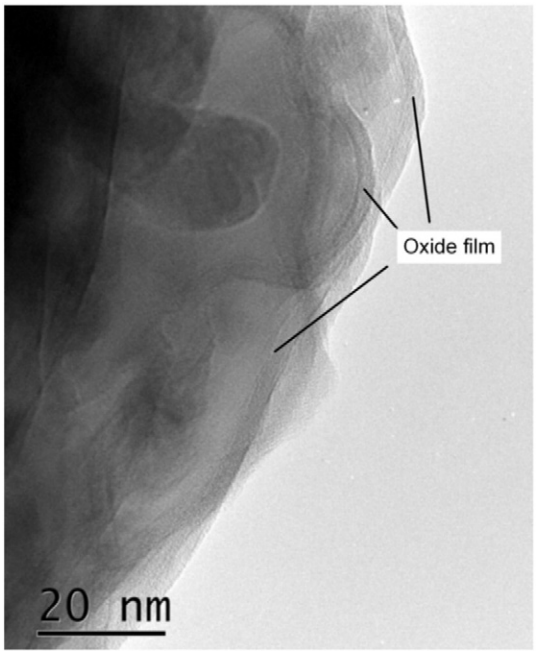

Fig. 9. Formed oxide films on the surface of the Al-Al_2O_3 composite powder.

percentage determined using Eq. (5) was 97.34%, the weight percentage of the O element was 2.66%. On the other hand, due to oxidation, a very thin oxide film had formed on the surfaces of the composite particles, and Fig. 9 shows at TEM image of the formed oxide films with a thickness of 3 nm. Due to the fact that the thickness of the oxide film was ultrathin, the weight of the O element from the film was relatively low and could be neglected when calculating the weight percentage of the O element. Thus, the results obtained from EDS mapping and Eq. (5) were considered to be consistent. Therefore, it can be concluded that the nano Al_2O_3 particulates were dispersed uniformly in the Al matrix after 20 h of milling.

4.4. Micro-hardness analysis

Fig. 10a shows a prepared micro-hardness testing specimen of the Al-Al_2O_3 composite powder ball-milled for 20 h. Optical microscopy inspections indicated that the composite powders were uniformly mounted in the phenolic resins. The obtained Vickers micro-hardness results are shown in Fig. 10b. It can be seen that the measured micro-hardness values of the raw Al varied from 49 HV0.05 to 58 HV0.05, and an average micro-hardness of 52.2 HV0.05 was thereby obtained.

Table 1
Atomic and weight fractions of the elements of the composite powder ball-milled for 20 h.

Element	Atomic %	Weight %
Al	96.08	97.64
O	3.92	2.36
Total	100	100

Compared to the raw Al, the obtained average Vickers hardness of the Al powder ball-milled for 20 h was 74.5 HV0.05. The significant increase in micro-hardness was closely correlated to the observed powder's microstructural evolution. More specifically, the broadened peaks in Fig. 6 indicated the Al grain refinement induced by high-energy ball milling and the TEM image in Fig. 7a verified that the Al grain size was refined and reduced to around 50 nm after 20 h of milling. The Al grain refinement resulted in the increase in the grain

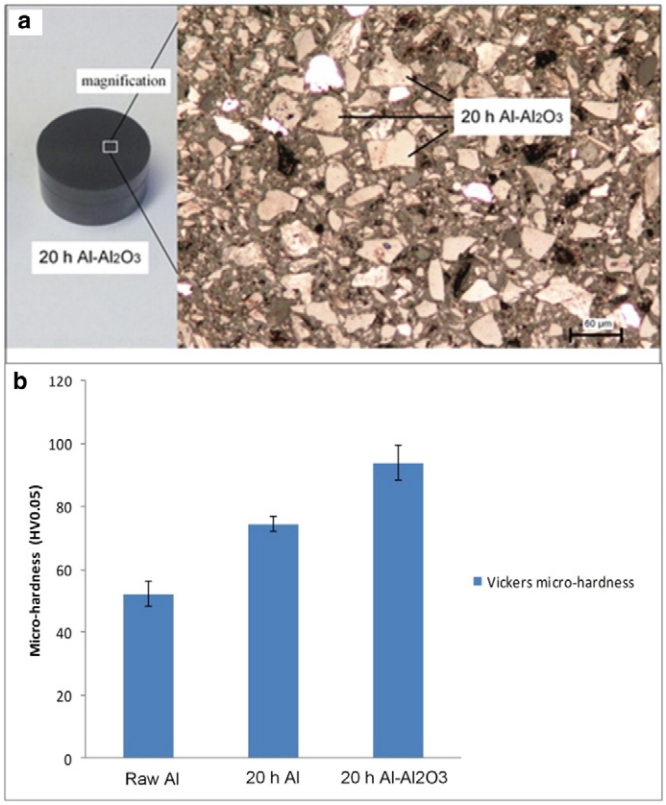

Fig. 10. Micro-hardness testing results.

boundaries, which thereby restricted dislocation motion and plastic deformation.

As for the Al-Al_2O_3 composite powder ball-milled for 20 h, the measured average micro-hardness increased by 26% in comparison with the Al powder ball-milled for 20 h. Likewise, this can also be explained by the powder's microstructural changes. In the first place, the observed FWHM of the 20 hour-milled composite powder was larger than that of 20 hour-milled Al powder (Fig. 6), which indicated the average grain size of the composite powder was smaller than the Al powder.

Moreover, the addition of the 4 vol.% nano Al_2O_3 reinforcement was another factor that resulted in the increase in hardness. The TEM image (Fig. 7b) and EDS spectrum (Fig. 8) indicated that the Al_2O_3 reinforcement was distributed uniformly amongst the Al matrix up to 20 h of milling. Further, the distance between Al_2O_3 particulates decreased with the continued milling process. Therefore, both the effect of the ball milling on the Al matrix and the effect of the Al_2O_3 reinforcement contributed to the increase in the hardness of the milled composite powder.

5. Conclusions and future research

This study explored the synthesis and characterisation of ball-milled Al-Al_2O_3 nanocomposite powder for additive layer manufacturing. It investigated the effect of milling and pause duration on the yield of Al-Al_2O_3 nanocomposite powder and employed advanced nanometrology methods and analytical techniques to study the characteristics of the composite powder. The following important findings derived from the results were presented in this paper:

(1) A combination of the short milling (10 min) and long pause (15 min) duration used in the high-energy ball milling process could generate a relatively high yield (66%) and narrow particle size distribution range of ball-milled composite powder, which would be suitable for SLM.
(2) SEM inspection showed that the composite powder ball-milled for 20 h provided more nearly spherical particles suitable for SLM than the Al powder milled for the same length of time. The measured Carr index of the composite and Al powders ball-milled for 20 h were 13.2% and 17.5%, respectively.
(3) Due to the very low volume fraction of Al_2O_3, only the Al phase was detected in the XRD spectrum of the ball-milled composite powder. The offset and shrinkage of the peaks of the composite powder indicated Al crystal structure transformation and proper Al_2O_3 embedding in the Al matrix when the milling continued for up to 20 h. TEM inspection, together with EDS analysis, verified the homogeneous dispersion of the Al_2O_3 in the Al matrix.
(4) The Vickers micro-hardness of the composite powder was 93.9 HV0.05, about a 26% increase in comparison with the Al powder ball-milled for 20 h.

The composite powder ball-milled for 20 h was considered to be suitable for selective laser melting due to its nearly spherical morphology, good flowability and high mechanical property. Nonetheless, the limitations of this study offer interesting directions for future studies. First, whilst a short milling and long pause combination generates a relative high yield for SLM, it consumes more working time and electrical energy. An optimum milling and pause combination should be determined to balance the yield and working efficiency. Second, whilst the ball-milled composite powder offers fine grains and great mechanical properties, the mechanical properties of the SLM-produced parts need to be investigated to a greater extent. Lastly, to obtain a better understanding of the advanced ball-milled Al-Al_2O_3 composite suitable for the SLM process, materials suppliers, machine manufacturers and academic researchers should ideally work together to provide a feasible solution.

Acknowledgements

The authors would like to thank Dr Emmanuel Brousseau and Dr Georgi Lalev from Cardiff University for the SEM and TEM operations and Mr Michael Bell from the University of Sheffield for the micro-hardness tests assistance. The lead author (Quanquan Han) gratefully appreciates the financial support of China Scholarship Council (CSC) and Cardiff University.

References

[1] S.M. Zebarjad, S.A. Sajjadi, Dependency of physical and mechanical properties of mechanical alloyed Al-Al2O3 composite on milling time, Mater. Des. 28 (2007) 2113–2120, http://dx.doi.org/10.1016/j. matdes.2006.05.020.
[2] A. Demir, N. Altinkok, F. Findik, I. Ozsert, The wear behaviour of dual ceramic particles (Al2O3/SiC) reinforced aluminium matrix composites, Key Eng. Mater. 264-268 (2004) 1079–1082, http://dx.doi.org/10.4028/www.scientific.net/KEM.264-268.1079.
[3] S. Tahamtan, A. Halvaee, M. Emamy, M.S. Zabihi, Fabrication of Al/A206-Al2O3 nano/micro composite by combining ball milling and stir casting technology, Mater. Des. 49 (2013) 347–359, http://dx.doi.org/10.1016/j.matdes.2013.01.032.
[4] S.M.S. Reihani, Processing of squeeze cast Al6061-30 vol% SiC composites and their characterization, Mater. Des. 27 (2006) 216–222, http://dx.doi.org/10.1016/j.matdes.2004.10.016.
[5] M.P. De Cicco, X. Li, L.S. Turng, Semi-solid casting (SSC) of zinc alloy nanocomposites, J. Mater. Process. Technol. 209 (2009) 5881–5885, http://dx.doi.org/10.1016/j.jmatprotec.2009.07.001.
[6] D. Bozic, B. Dimcic, O. Dimcic, J. Stasic, V. Rajkovic, Influence of SiC particles distribution on mechanical properties and fracture of DRA alloys, Mater. Des. 31 (2010) 134–141, http://dx.doi.org/10.1016/j.matdes.2009.06.047.
[7] A. Mazahery, H. Abdizadeh, H.R. Baharvandi, Development of high-performance A356/nano-Al2O3 composites, Mater. Sci. Eng. A 518 (2009) 61–64, http://dx.doi.org/10.1016/j.msea.2009.04.014.
[8] T.G. Durai, K. Das, S. Das, Synthesis and characterization of Al matrix composites reinforced by in situ alumina particulates, Mater. Sci. Eng. A 445-446 (2007) 100–105, http://dx.doi.org/10.1016/j. msea.2006.09.018.
[9] Y.C. Kang, S.L.I. Chan, Tensile properties of nanometric Al2O3 particulate-reinforced aluminum matrix composites, Mater. Chem. Phys. 85 (2004) 438–443, http://dx.doi.org/10.1016/j. matchemphys.2004.02.002.
[10] D. Poirier, R.A.L. Drew, M.L. Trudeau, R. Gauvin, Fabrication and properties of mechanically milled alumina/aluminum nanocomposites, Mater. Sci. Eng. A. 527 (2010) 7605–7614, http://dx.doi.org/10.1016/j.msea.2010.08.018.
[11] R.B. Patil, V. Yadava, Finite element analysis of temperature distribution in single metallic powder layer during metal laser sintering, Int. J. Mach. Tools Manuf. 47 (2007) 1069–1080, http://dx.doi.org/10.1016/j.ijmachtools.2006.09.025.
[12] S.P. Soe, D.R. Eyers, R. Setchi, Assessment of non-uniform shrinkage in the laser sintering of polymer materials, Int. J. Adv. Manuf. Technol. 68 (2013) 111–125, http://dx.doi.org/10.1007/s00170-012-4712-0.
[13] D.D. Gu, W. Meiners, K. Wissenbach, R. Poprawe, Laser additive manufacturing of metallic components: materials, processes and mechanisms, Int. Mater. Rev. 57 (2012) 133–164, http://dx.doi.org/10.1179/1743280411Y.0000000014.
[14] N. Altinkok, T. Ozsert, F. Findik, Dry sliding wear behavior of Al2O3/SiC particle reinforced aluminum based MMCs fabricated by stir casting method, Acta Phys. Pol. A. 124 (2013) 11–19. doi: 10.12693/APhysPolA.124.11.
[15] A.S. Khan, B. Farrokh, L. Takacs, Effect of grain refinement on mechanical properties of ball-milled bulk aluminum, Mater. Sci. Eng. A 489 (2008) 77–84, http://dx.doi.org/10.1016/j.msea.2008.01.045.
[16] S.S. Razavi Tousi, R. Yazdani Rad, E. Salahi, I. Mobasherpour, M. Razavi, Production of Al-20 wt.% Al2O3 composite powder using high energy milling, Powder Technol. 192 (2009) 346–351, http://dx.doi.org/10.1016/j.powtec.2009.01.016.
[17] J. Liao, M.-J. Tan, Mixing of carbon nanotubes (CNTs) and aluminum powder for powder metallurgy use, Powder Technol. 208 (2011) 42–48, http://dx.doi.org/10.1016/j.powtec.2010.12.001.
[18] D.R. Amador, J.M. Torralba, Morphological and microstructural characterisation of low-alloying Fe powder obtained by mechanical attrition, J. Mater. Process. Technol. 143–144 (2003) 776–780, http://dx.doi.org/10.1016/S0924-0136(03)00372-8.
[19] D.L. Zhang, Processing of advanced materials using high-energy mechanical milling, Prog. Mater. Sci. 49 (2004) 537–560, http://dx.doi.org/10.1016/S0079-6425(03)00034-3.
[20] B. Prabhu, C. Suryanarayana, L. An, R. Vaidyanathan, Synthesis and characterization of high volume fraction Al-Al2O3 nanocomposite powders by high-energy milling, Mater. Sci. Eng. A 425 (2006) 192–200, http://dx.doi.org/10.1016/j.msea.2006.03.066.
[21] S.M. Zebarjad, S.A. Sajjadi, Microstructure evaluation of Al-Al_2O_3 composite produced by mechanical alloying method, Mater. Des. 27 (2006) 684–688, http://dx.doi.org/10.1016/j.matdes.2004.12.011.
[22] M.T. Khorshid, S.A.J. Jahromi, M.M. Moshksar, Mechanical properties of tri-modal Al matrix composites reinforced by nano- and submicron-sized Al2O3 particulates developed by wet attrition milling and hot extrusion, Mater. Des. 31 (2010) 3880–3884, http://dx.doi.org/10.1016/j. matdes.2010.02.047.
[23] H. Su, W. Gao, Z. Feng, Z. Lu, Processing, microstructure and tensile properties of nano-sized Al2O3 particle reinforced aluminum matrix composites, Mater. Des. 36 (2012) 590–596, http://dx.doi.org/10.1016/j.matdes.2011.11.064.

[24] E. Emery, J. Oliver, T. Pugsley, J. Sharma, J. Zhou, Flowability of moist pharmaceutical powders, Powder Technol. 189 (2009) 409–415, http://dx.doi.org/10.1016/j.powtec.2008.06.017.
[25] A. Nokhodchi, M. Maghsoodi, D. Hassan-Zadeh, M. Barzegar-Jalali, Preparation of agglomerated crystals for improving flowability and compactibility of poorly flowable and compactible drugs and excipients, Powder Technol. 175 (2007) 73–81, http://dx.doi.org/10.1016/j. powtec.2007.01.030.
[26] I. Yadroitsev, Selective Laser Melting: Direct Manufacturing of 3D-objects by Selective Laser Melting of Metal Powders, Lambert Academic Publishing, Saarbrucken, 2009.
[27] H.J. Choi, S.W. Lee, J.S. Park, D.H. Bae, Tensile behavior of bulk nanocrystalline aluminum synthesized by hot extrusion of ball-milled powders, Scr. Mater. 59 (2008) 1123–1126, http://dx.doi.org/10.1016/j.scriptamat.2008.07.030.